VOL. 11, NO. 1, JANUARY 2016 ISSN 1819-6608
ARPN Journal of Engineering and Applied Sciences

www.arpnjournals.com

AN IMPROVED METHOD TO MODEL SEMI-ELLIPTICAL SURFACE CRACKS USING ELEMENT MISMATCH IN ABAQUS

R. H. A. Latiff and F. Yusof
School of Mechanical Engineering, UniversitiSains, Malaysia
E-Mail: mefeizal@usm.my

ABSTRACT

The purpose of this paper is to propose and investigate the feasibility of using multiple element types in a single model, termed element mismatch, for a three-dimensional semi-elliptical crack problem. The purpose behind the exploration of this method is to ease the meshing process in complex models. Multiple semi-elliptical surface crack in tension models were created with single element mesh and multi-elementmeshes with different mesh densities. It was found that the element mismatch modelsdeveloped a consistent stress intensity factor for all the applied loading and geometries. When compared to the single element type models, the computation times were found to be significantly lower for the element mismatch models and the results were largely independent of mesh density.

Keywords: fracture mechanics, abaqus, element mismatch.

INTRODUCTION

The optimum use of computational resources for a finite element numerical analysis is an important issue in computational fracture mechanics [1]. As the accuracy of crack-tip deformation problem becomes critical, the crack tip mesh nodal and elemental configurations will usually be increased, which will directly increase the time to complete the analysis due to large degrees of freedom. However this approach may not give an accurate outcome. For structural problems, the sizing of the elements using the h method [2] or p method [3] to revise finite element meshes to obtain the necessary accuracy by using as many degrees of freedom as necessary, also called adaptive meshing, has been introduced. However problems with geometrical discontinuities, such as cracks, may not developed convergence of solution appropriately.

Three-dimensional elastic-plastic crack tip problems have evolved over 40 years from the defining work of[4]. The development of formulation for three-dimensional elastic-plastic crack tip problems gained momentum after efficient finite element formulation was combined with the computing capability to handle problems with a large number of degrees of freedom in the eighties[5, 6]. However, the results were partially inconclusive with respect to their original hypothesis of a plane stress field at the region where the crack front approached the free surface. A widely accepted three-dimensional elastic crack tip formulation breakthrough came through the work of [7]. However, the three-dimensional elastic-plastic crack tip formulation [8] was not able to capture the sensitivity of the corner field effect due to mesh inadequacy at the free surface. Three-dimensional elliptical surface crack was discussed by [9] but was limited in the crack configuration and material response, while recent work by[10] was also limited to unvarying crack configurations due to complexity of the problem.

Presently, commercially available FEA codes, such as ABAQUS[11],are widely used to elucidate the nature of crack tip stress strain behaviour quite successfully. ABAQUS incorporates fracture mechanics in its library of functions and analysis tools. However, ABAQUS has limited the region around the crack front toonly certain types of elements, specifically quadrilateral elements in two-dimensional models and hexahedral brick elements in three-dimensional models [11]. Due to this limitation, fracture mechanics models typically used a single type of element for the entire model. However, [12] has undertaken work to model the crack front using non-brick elements.

UsingABAQUS/CAE, the regions outside of the crack front can be meshed using other than the brick type of element. A quadratic brick element has 20 nodes while a quadratic tetrahedral element has 10 nodes and a quadratic wedge element has 15 nodes. The use of elements with fewer nodes, and thus fewer degrees of freedom (DOF), in the regions outside of the crack front would allow for models to be solved with shorter computing times. Furthermore, meshing of complex bodies is relatively difficult using brick elements as meshing requires careful partitioning of the model. In fracture mechanics, one such model is the semi-elliptical surface crack which requires partitioning before structured meshing using brick elements was allowed by ABAQUS, as shown in Figure-1 below.

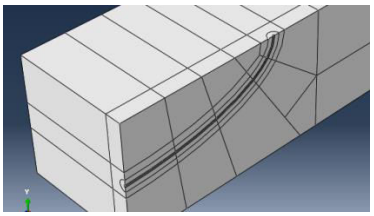

Figure-1. Partitioning of a semi-elliptical surface crack quarter model.

Element mismatch, henceforth EM, refers to the condition where a mesh comprises of multiple element types. Two types of meshes incorporating EM can be created using ABAQUS. The first type of mesh createsa single continuous mesh using different elements, while the second type of mesh creates separate meshes for each of the element types.In a continuous mesh, interface nodes are shared by the neighbouring elements, as shown in Figure-2, where Triangular elements share nodes with Quadrilateral elements. The limitation to this method is that the elements must have compatible edge and surface node configurations. For example, the Quadrilateral and Triangular elements in Figure-2 have compatible edge node configurations; both elements have two nodes per edge. Thus they can be meshed as a continuous mesh.

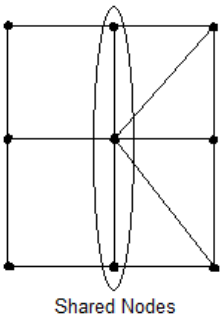

Figure-2. Elements of differing types sharing nodes.

The requirement of having matching node configurations on edges also applies to 3D modelling. The surfaces of the elements must match in order for ABAQUS to generate a continuous mesh. Thus, not all elements are compatible. For example, the surfaces of a brick element and a tetrahedral element have no matching surfaces, as shown in Figure 3. The brick element has 8 nodes per surface while the tetrahedral element only has 6nodes per surface. However, wedge elements share compatible surfaces with brick elements, as highlighted in Figure-3.

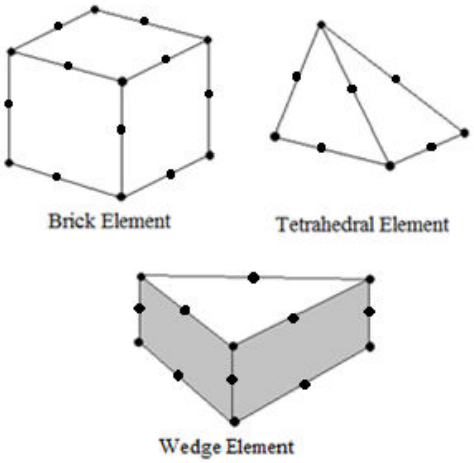

Figure-3. Linear brick and tetrahedral element configurations.

As previously discussed, another method for incorporating EM into a finite element model is the creation of separate meshes using different elements. These meshes can be configured to behave as a continuous mesh via the Tie Constraint provided in ABAQUS/CAE. The elements in this configuration do not share nodes, as shown in Figure 4. The authors of [13]have done some work using the Tie Constraint and XFEM for fracture mechanics. The use of the Tie Constraint is not discussed in this paper, as it generates a discontinuous mesh.

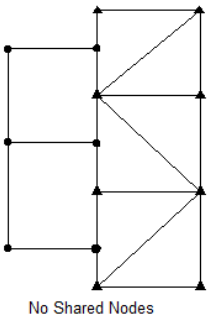

Figure-4. Tie constrained elements.

This paper investigates the feasibility of using EM within a single continuous mesh for fracture mechanics purposes. Emphasis was given to accuracy of the results and also the computing time required in performing the analysis. The scope of this paper is limited to an elastic stationary semi-elliptical surface crack under tension.

METHODOLOGY

A semi-elliptical surface crack in tension was modelled using ABAQUS/CAE. To investigate the feasibility of using EM in fracture mechanics, models incorporating EM and standard single element type meshes were used. The stress intensity factor K of the models were determined and compared to the equation provided by[14]:

$$K = (S_t)\sqrt{\pi \frac{a}{Q}} F(\frac{a}{t}, \frac{a}{c}, \frac{c}{b}, \varphi) \quad (1)$$

Where S_t is the remote tensile stress, and F and Q are functions of the geometry of the specimen.

The models created share a single geometry, as shown in Table-1 and Figure-5. Figure-5(a) also indicates the lines of symmetry. Figure-5(b) shows the angular system used to discuss the results in the Discussion section. The depth of surface crack *a*, the half-width of the cracked plate *b*, the half-length of surface crack *c*, the plate thickness *t*, and the parametric angle of the ellipse φ are indicated in Figure-5.

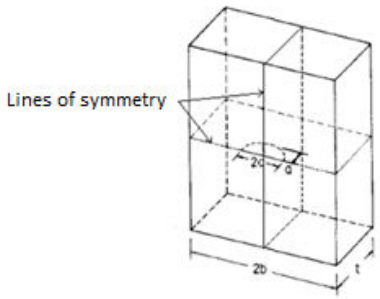

(a)

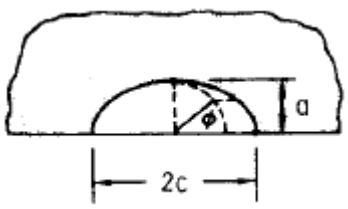

(b)

Figure-5. Semi-elliptical surface cracked plate[14].

Table-1. Geometry configurations based on Figure-5.

Geometric ratios	Value
a/t	0.5
a/c	0.4
c/b	0.325

Wedge elements were chosen for the for the EM mesh as they have a compatible surface with brick elements, as show in Figure 3.The element types used in the analyses are reduced-integration quadratic brick elements(C3D20R) and reduced integration quadratic wedge elements(C3D15). The K valuesof the models were benchmarked to (1). A comparison of the accuracy of the results and computation time were made.

Finite element models

Due to symmetry, as shown in Figure 5(a), the analysis was conducted based ona quarter model framework. A tensile load was applied to the models using displacement, $u_1$as shown in Figure 6 while symmetrical conditions were enforced for the x and z axes.

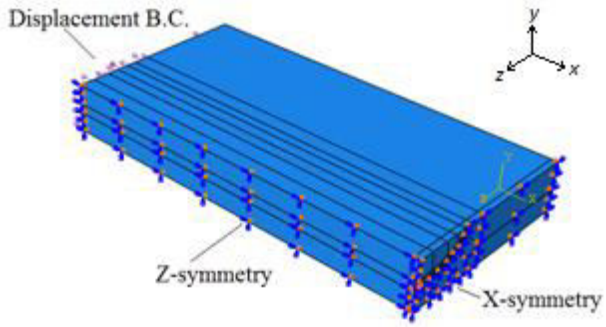

Figure-6. Boundary conditions for all models.

To investigate the effects of EM, two types of models were created and compared, with one incorporating EM and another model using only brick elements. Both models share the same crack front configuration in terms of element type and element sizes. In both models, the crack fronts were meshed with brick elements, as per the limitation set by ABAQUS. The remaining sections of the models were meshed differently. In the 'Brick models,' the entire model was meshed with brick elements while in the 'EM models', the remaining sections of the models were meshed with wedge elements. This is shown in Figure 7. Four crack fronts with varying mesh densities were also modelled to further investigate the effects of EM. Thus, a total of 8 models were used for the study.

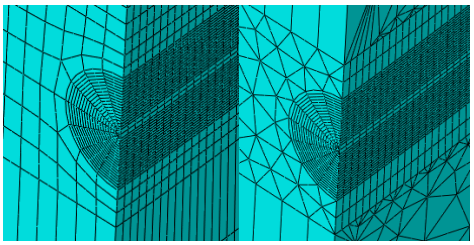

(a) (b)

Figure-7. a) Brick element and b) Element mismatch meshes

Table-2 below indicates the configurations for each of the models used. The naming convention for the models is such that the brick models are denoted with 'B' in their names, while the EM models are denoted with 'M'. The numbering indicates therelative density of the mesh at the crack front, with '4' indicating the finest mesh at the crack front. Thus, B1 and M1 have the same crack front mesh, as do B2 and M2, and so on.

Table-2. Mesh configurations.

Name	Elements used	No. DOF
B1	C3D20R	98,151
B2	C3D20R	160,188
B3	C3D20R	510,171
B4	C3D20R	433,173
M1	C3D20R, C3D15	73,953
M2	C3D20R, C3D15	87,138
M3	C3D20R, C3D15	217,950
M4	C3D20R, C3D15	249,087

The meshes outside of the crack front were intentionally designed to becoarse in comparison to the crack front. The mesh seeding for the models were manually adjusted until the elements within the mesh did not exceed the built-in aspect ratio limits. The models using solely brick elements have a greater number of DOF. This occurred as it is relatively easy to transition from a fine mesh to a rough mesh using a wedge element when compared to a brick element without exceeding the built in aspect ratio in ABAQUS, as shown in Figure 8. This was done to indicate that the roughness of the mesh outside the crack front region did adversely affect the results, as presented in the following section.

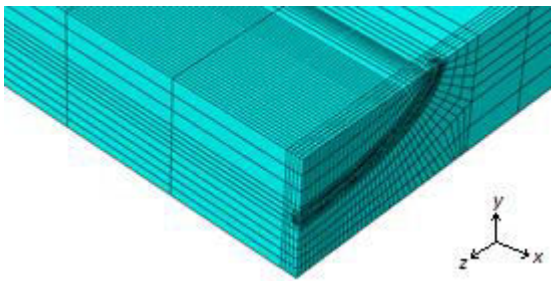

(a)

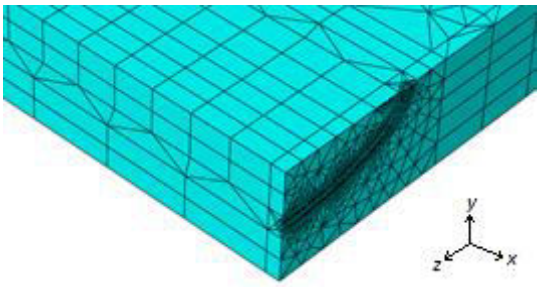

(b)

Figure-8. Comparison of transitioning mesh densities

RESULTS AND DISCUSSIONS

Figures 9 and 10 show K of the brick element models and models incorporating EM compared to the benchmark results by [14]. The angles indicated in the figures are based of the notation used in Figure-5(b).

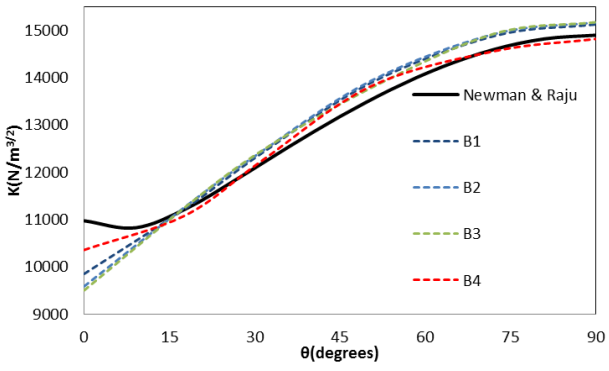

Figure-9. SIF of B1-B4.

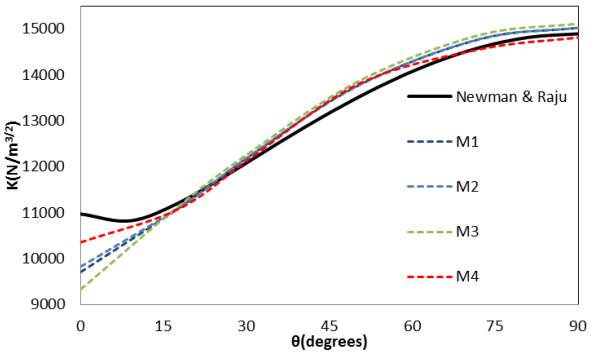

Figure-10. SIF of M1-M4.

Benchmarking

Referring to Figures 9 and 10, K of the models were generally in good agreement with the work by [14]. The percentage differences for all models when compared to [14] were found to remain below 3% between the 20º to 90º range. However, the percentage difference increased below the 20º angle. The percentage difference reached a maximum of 15% at the 0º angle for the B1 and M1 models.

It should be noted that the meshing density around the crack tip appears to have affected the results of the analysis. The maximum percentage difference, occurring at the 0º angle in all cases, showed a marked decrease with increasing crack tip mesh density. The models with the densest mesh at the crack front were B4 and M4. Both exhibited a percentage difference of 5.6%. Thus, the higher percentage difference at the 0º angle can be reduced via a finer mesh around the crack front. In both the brick element and EM models, more accurate K values were achieved with increasing mesh density around the crack front.

Referring to Table-3, the number of DOF for M4 was much lower than the number of DOF for B3. It must be noted that the values in Table 3 refer to the DOF of the entire model. Although experience suggests that a denser mesh would return more accurate results, the K values for M4 are more accurate than B3 at the 0º angle. This further proves that the mesh around the crack front is more crucial to the accuracy of the results than the mesh in other regions.

Table-3. DOF comparison.

Brick model	DOF	EM model	DOF	% reduction of DOF
B1	98,151	M1	73,953	24.7
B2	160,188	M2	87,138	45.6
B3	510,171	M3	217,950	57.3
B4	433,173	M4	249,087	42.5

Comparing the K values between the brick element models and EM models in Figures 9 and 10, the results do not vary by a significant margin, approximately by 2%. Here, we can infer that K is largely unaffected by the use of EM. The results of the analysis can be further improved to fit the benchmark by increasing the mesh density around the crack front.

Thus, EM appears to be a feasible alternative to meshing in fracture mechanics analyses as K was more heavily influenced by the mesh around the crack tip as opposed to the mesh outside of the crack tip.

Computation time

Referring to Table-3, the number of DOF for the EM models was fewer than their counterpart brick element models. As the meshes around the crack front compared were the same, the reduction in number of DOF was a result of the mesh outside of the crack front. This is due to the ease in which wedge elements are able to transition from a dense mesh to a course mesh when compared to brick elements, as previously shown in Figure 8. Despite the fewer DOF, the results were not adversely affected, as previously discussed.

A comparison of the computation times shown in Table-4 confirms that the analysis of the EM models required less time when compared to the brick element models. In the most accurate of the models, the B4 and M4 models, the reduction of computation time from the B4 model to the M4 model was 37%. This reduction corresponds to a 42.5% reduction in the number of DOF. This was to be expected as the computation time is linked to the number of degrees of freedom. This is a good indication that computing times for fracture mechanics models can be significantly reduced via the implementation of EM, at least within the elastic paradigm.

Table-4. Computation time comparison.

Brick model	CPU time	EM model	CPU time	% reduction of CPU time
B1	51.2	M1	25.9	49.4
B2	129.4	M2	36.4	71.9
B3	1363.8	M3	264.1	80.6
B4	1291.8	M4	813.6	37

Table-4 shows that the reduction of computing time is significant without much loss from the results, as shown in Figures 9 and 10. This indicates that incorporating EM is a feasible approach for fracture mechanics simulation, within an elastic material response.

CONCLUSIONS

Models of elastic semi-elliptical surface cracks were built and meshed in various configurations. It was found that the results of the EM models and [14] are in good agreement. The computation times for the mismatch models were significantly decreased, when compared to the brick element models. Thus, the implementation of Element Mismatch (EM) is viable in the simulation of stationary cracks.

FURTHER WORK

1. To investigate effects of Tetrahedral elements in element mismatch on fracture mechanics model.
2. To update models to include an elastic-plastic response.
3. To determine the effects of element mismatch & tie constraint on both elastic and elastic-plastic fracture mechanics model.

ACKNOWLEDGEMENTS

The authors would like to acknowledge the MOHE grant (FRGS/1/2014/TK01/USM/02/5) which funded this research project. The ABAQUS finite element code that was used to perform the analyses was made available under an academic license from Dassault Systemes, K. K. Japan.

REFERENCES

[1] M. Kuna, "Finite Elements in Fracture Mechanics," Theory–Numerics–Applications. Solid Mechanics and Its Applications, vol. 201, 2013.

[2] L. Demkowicz, P. Devloo, and J. T. Oden, "On an h-type mesh-refinement strategy based on minimization of interpolation errors," Computer Methods in Applied Mechanics and Engineering, vol. 53, pp. 67-89, 1985.

[3] O. Zienkiewicz, C. Emson, and P. Bettess, "A novel boundary infinite element," International Journal for Numerical Methods in Engineering, vol. 19, pp. 393-404, 1983.

[4] N. Levy, P. Marcal, and J. Rice, "Progress in three-dimensional elastic-plastic stress analysis for fracture mechanics," Nuclear Engineering and Design, vol. 17, pp. 64-75, 1971.

[5] W. Brocks and J. Olschewski, "On J-dominance of crack-tip fields in largely yielded 3D structures," International Journal of Solids and Structures, vol. 22, pp. 693-708, 1986.

[6] G. W. Wellman, S. T. Rolfe, and R. H. Dodds, "Three-dimensional elastic-plastic finite element analysis of three-point bend specimens," ASTM STP, vol. 868, pp. 214-237, 1985.

[7] T. Nakamura and D. Parks, "Three-dimensional stress field near the crack front of a thin elastic plate," Journal of applied Mechanics, vol. 55, pp. 805-813, 1988.

[8] T. Nakamura and D. Parks, "Three-dimensional crack front fields in a thin ductile plate," Journal of the Mechanics and Physics of Solids, vol. 38, pp. 787-812, 1990.

[9] Y. Wang, "A two-parameter characterization of elastic-plastic crack tip fields and applications to cleavage fracture," Massachusetts Institute of Technology, 1991.

[10] O. Terfas, "Quantification of Constraint in Three-Dimensional Fracture Mechanics," Doctor of Philosphy, Department of Mechanical Engineering, University of Glasgow, 2010.

[11] A. Version, "6.13," Analysis User's Guide, Dassault Systems, 2013.

[12] M. Nejati, A. Paluszny, and R. W. Zimmerman, "On the use of quarter-point tetrahedral finite elements in

linear elastic fracture mechanics," Engineering Fracture Mechanics. vol. 144, pp. 194-221, 2015.

[13] M. Levén and R. Daniel, "Stationary 3D crack analysis with Abaqus XFEM for integrity assessment of subsea equipment," 2012.

[14] J. Newman and I. Raju, "An empirical stress-intensity factor equation for the surface crack," Engineering Fracture Mechanics. vol. 15, pp. 185-192, 1981.